

Meshless Local Petrov-Galerkin Method with Unity Test Function for Non-Isothermal Fluid Flow

A. Arefmanesh¹, M. Najafi¹ and H. Abdi¹

Abstract: The meshless local Petrov-Galerkin (MLPG) method with unity as the weighting function has been applied to the solution of the Navier-Stokes and energy equations. The Navier-Stokes equations in terms of the stream function and vorticity formulation together with the energy equation are solved for different test cases. This present study considers the implementation of the method on a non-isothermal lid-driven cavity flow, the lid-driven cavity flow with an inlet and outlet, and also on the non-isothermal flow over an obstacle. Nonuniform point distribution is employed for all the test cases for the numerical simulations. The flow streamlines for each test case is depicted. The L^2 -norm of the error as a function of the size of the control volumes is presented for moderate Reynolds numbers and the rate of convergence of the method is established. Close agreements of the obtained results with those of the other numerical techniques show that the proposed method is applicable in solving a variety of non-isothermal fluid flow problems.

Keyword: meshless, control volume, Petrov-Galerkin, stream function, vorticity

Nomenclature

h distance between two consecutive points
 L domain length
 N total number of points
 P pressure
 Pe Peclet number
 q heat flux
 R radius
 Re Reynolds number
 T temperature

U lid velocity
 V velocity
 w weighting function

Greek Symbols

α thermal diffusivity
 ϕ interpolation function
 Γ boundary
 Γ_g, Γ_h boundary segments
 ν kinematic viscosity
 ρ density
 Ω domain
 ω vorticity
 ψ stream function

Subscripts

i point or control volume number
 BW bottom wall
 TW top wall
 x x-derivative

Superscripts

* physical variable
 $-$ dimensionless variable, balancing coefficient
 \wedge unit vector
 $+$ local variable
 \rightarrow vector

1 Introduction

Various meshless schemes have been introduced in recent years in order to circumvent the difficulties associated with mesh generation in the well-established numerical techniques, such as the finite element and the finite volume methods [Atluri and Shen (2002); Atluri (2004)]. Among the earliest so-called meshless techniques is “the

¹ Islamic Azad University, Science & Research Branch, Tehran, Iran

diffuse element method” proposed by Nayroles, Touzot and Villon (1992) in which a collection of nodes and a boundary description are sufficient to obtain the Galerkin equations. However, in this method, an auxiliary grid is still required to evaluate the integrals which result from applying the Galerkin method to the differential equations. Subsequently, via introducing a regular cell structure as the auxiliary grid, Belytschko, Krongauz, Organ, Flemming and Krystel (1996) and Lu, Belytschko and Gu (1994) transformed the above technique to the so-called element-free Galerkin method.

In recent years, two other meshless technique – the meshless local boundary equation method, and the meshless local Petrov-Galerkin method (MLPG)– have been proposed by Zhu, Zhang and Atluri (1998) and Atluri and Zhu (2000), respectively. In these schemes, a local weak form of the differential equation over a local subdomain together with the shape function from moving least-squares (MLS) interpolations are used to obtain the discretized equations. A recent comprehensive review of the MLPG method with emphasis on the solid mechanics applications can be found in Atluri’s book (2004).

Among other developments in the area of meshless techniques, one can mention the method of spheres proposed by De and Bathe (2001), in which subdomains of spherical shapes are generated at every point in the domain. Subsequently, the dependant variables are interpolated within the spheres and the discretized equations are obtained by substituting the interpolations in the Galerkin weak form of the differential equation for the subdomains. Other truly meshless scheme that have been recently proposed and applied specifically to elasticity problems are the local point interpolation method by Gu and Liu (2001), the regular hybrid boundary node method by Zhang and Yao (2004), and a modified meshless local Petrov-Galerkin method to elasticity problems in computer modeling and simulation by Hu, Long, Liu and Li (2006). In this work [Hu, Long, Liu and Li (2006)], the MLPG method is implemented using the moving least squares approximation. Heaviside test function is chosen to

overcome the computational costs, and essential boundary conditions are imposed by using a direct interpolation method. A comparison study of the efficiency and accuracy of a variety of MLPG methods is made in a study by Atluri and Shen (2002). In this study, different test functions resulted different MLPG methods. In order to develop a fast and robust meshless method, ways to avoid the use of a domain integral in the weak-form, by choosing an appropriate test function were explored. Convergence studies of the numerical examples showed that all of the MLPG methods possessed excellent rates of convergence for both the unknown variables and their derivatives. The analysis of computational costs showed that the proposed MLPG method was less expensive in computational costs as well as in human-labor costs compared to finite element and boundary element methods.

Applications of the MLPG method on solid mechanics area are substantial. In a work by Vavourakis and Polyzos (2007), the use of derivatives of the MLS shape functions were avoided through treating displacements and stresses as independent variables through the corresponding local integral equations and considering nodal points located only internally and externally and not on the global boundary of the analyzed elastic structure. In a study by Han and Atluri (2004), three different MLPG methods (using different test functions) were developed for solving three-dimensional elastostatic problems. A novel definition of the local three-dimensional subdomain was presented in order to perform the numerical integration accurately. Atluri, Han and Rajendran, (2004) introduced a meshless finite volume method by taking the Heaviside function as the test function for solving elastostatic problems. A new MLPG method called singular/hypersingular MLPG method was developed by Sellountos, Vavourakis and Polyzos (2005) based on local boundary integral equation (LBIE) for solving elastostatic problems. In this work strong singular and hypersingular integrals were evaluated directly and with high accuracy by means of advanced integration techniques. Comparison studies on the accuracy provided by five different elas-

stostatic MLPG type formulations, based on LBIE, were made by Vavourakis, Sellountos and Polyzos, (2006). Useful conclusions on the accuracy and the stability of an MLPG (LBIE) method were also addressed. Sladek J., Sladek V. and Atluri (2004) proposed an MLPG method for static and elastodynamic problems in a homogenous and anisotropic medium using Heaviside step function as the test function in the local weak form. The final form of local integral equations has a pure contour character only in elastostatics. In elastodynamics an additional domain integral is involved due to inertia terms. A non-linear formulation of the MLPG finite volume mixed method was developed for the large deformation analysis of static and dynamic problems of large deformations and rotations of a hyper-elastic cantilever beam, and impact of an elasto-plastic solid rod on a rigid surface [Han, Rajendran and Atluri (2005)]. The work showed that the mixed MLPG method was relatively more efficient than the FEM for the examples considered. In a work by Atluri, Liu and Han (2006), an MLPG mixed collocation method was proposed for solving elasticity problems. In the MLPG approach, the mixed scheme was applied to interpolate the displacements and stresses independently. The numerical examples showed that the proposed MLPG mixed collocation method possessed a stable convergence rate, and was more efficient than the other MLPG implementations, including the MLPG finite volume method. A mixed finite difference MLPG method was proposed for solving a number of solid mechanics problems [Atluri, Liu and Han (2006)]. A mixed interpolation scheme was also adopted in the implementation: the displacements, displacement gradients, and stresses were interpolated independently using identical MLS shape functions. Numerical examples showed that the proposed MLPG mixed finite difference method was accurate and efficient.

In a study by Sladek J., Sladek V., Wen and Aliabadi (2006), an MLPG method was applied to solve bending problems of shear deformable shallow shells described by the Reissner theory. For transient elastodynamic case the Laplace-transform was used to eliminate the time de-

pendence of the field variables. The meshless approximation based on the MLS method was employed for the implementation. Unknown Laplace-transformed quantities were computed from the local boundary integral equations. The time-dependant values were obtained by the Stehfest's inversion technique. A meshless computational method based on the local Petrov-Galerkin approach for the analysis of shell structures was presented by Jarak, Sori'c and Hoster (2007). A concept of a three dimensional solid allowing the use of completely 3-D constitutive models was applied. Discretization was carried out by using both a MLS approximation and polynomial functions. The numerical efficiency of the derived concept was demonstrated by numerical examples. In a work by Han and Atluri (2004), an MLPG method was developed for solving 3-D elastodynamic problems. The numerical technique in this work imposes a correction to all accelerations, to enforce the kinematic boundary conditions in the MLS approximation, while using an explicit time-integration algorithm. An efficient meshless formulation based on the local Petrov-Galerkin approach for the analysis of shear deformation over the thickness was used for the in-plane displacements, while the hierarchical quadratic interpolation was adopted by Sori'c, Li, Jarak and Atluri, (2004) for the transversal displacement in order to avoid the thickness locking effect. The implementation of a three-dimensional dynamic code, for contact, impact, and penetration mechanics based on the MLPG was presented by Han, Liu, Rajendran and Atluri (2006). The computational times for the simulations made were also recorded, and were compared with those of the popular finite element code (Dyna3D), to demonstrate the efficiency of implemented approach. In a work by Sladek J., Sladek V., Zhang, Solek and Starek (2007), a meshless method based on the local Petrov-Galerkin approach was proposed for crack analysis in two-dimensional and three-dimensional axisymmetric piezoelectric solids with continuously varying material properties. The accuracy of the proposed method for computing the stress intensity factor (SIF) and electrical displacement intensity factor (EDIF) were discussed by comparison

with available analytical or numerical solutions. A meshless method based on the local Petrov-Galerkin approach was proposed for the solution of boundary value problems for coupled thermo-electro-mechanical fields [Sladek J., Sladek V., Zhang and Sulek (2007)]. Transient dynamic governing equations were considered and to eliminate the time-dependence, the Laplace-transform technique was applied. Two-dimensional analyzed domain was subdivided into small circular sub-domains surrounding nodes randomly spread over the whole domain. A unit step function was used as the test function. The moving MLS method was adopted for the approximation of the physical quantities. The Stehfest's inversion method was applied to obtain the final time-dependent solutions. An MLPG method for studying the diffusion of a magnetic field within a non-magnetic conducting medium with non-homogeneous and anisotropic electrical resistivity was proposed by Johnson and Owen (2007). The method has the potential to be combined with other mesh-free methods such as smoothed particle hydrodynamics (SPH) to solve problems in resistive magneto-hydrodynamics. It must be emphasized here that a good number of other studies on different aspects, and applications of MLPG are made by the authors mentioned in this work, and also by some other authors such as S. Shen, J. Krivacek, Ch. Zhang, U. Andreaus, L. Gao, K. Liu, Y. Liu, R. Pecher, W. Yuan, P. Chen, and many others.

There are also some recent developments in the applications of meshless techniques to fluid flow and heat transfer problems. Lin and Atluri (2000, 2001), in two different works, used the MLPG method to solve convection-diffusion problems as well as the Navier-Stokes (N-S) equations. They introduced different upwinding schemes and modified the local weak form so as to overcome the so-called Babuska-Brezzi conditions while solving the N-S equations. The MLPG method has been implemented for solving steady as well as transient heat conduction problems in a continuously non-homogeneous anisotropic medium [Sladek J., Sladek V. and Atluri (2004)]. In this work, Heaviside step function together with moving least-squares method has been employed to

obtain the discretized equations. Wu, Shen and Tao (2007) have applied the MLPG collocation method to two-dimensional heat conduction problems in irregular domain. The results show that the method is in good agreement with standard existing packages, and it can accurately describe the boundaries of irregular domain. A thermo-mechanical analysis of functionally graded composites under laser heating has been conducted using the MLPG method. Numerical results are presented for the thermomechanical responses in both the steady and transient states [Ching and Chen (2006)]. Recently the MLPG method based on Rankine source solution has been implemented for simulating nonlinear water waves generated by wavemakers [Ma (2005)]. In this study the solution for Rankine source was taken as the test function and the local weak form was expressed in terms of pressure rather than pressure gradient. Arefmanesh, Najafi and Abdi (2005) have applied a variation of the MLPG method with unity as the test function to the convection-diffusion, and potential flow equations. The results show that the method combined with a proper upwinding scheme is very promising for obtaining accurate solutions to problems in the field of thermofluids. Also in a very recent work Liu (2006) has used an MLPG approach based on discrete-ordinate equations to solve a radiation heat transfer problem in multi-dimensional absorbing-emitting-scattering semitransparent graded index media. His results show that the MLPG method gives good accuracy in solving radiation heat transfer problems.

In this present study, the meshless local Petrov-Galerkin method with unity as the test function is applied to the solutions of the non-isothermal viscous flow equations. A variation of the streamline upwind Petrov-Galerkin (SUPG) technique based on adding optimal balancing diffusion along the streamlines is employed to obtain a stable solution for high Peclet, and moderate Reynolds numbers. To establish the rate of convergence of the method, wherever possible, the L^2 -norm of the error is presented.

2 Numerical model

A bounded region Ω with the boundary $\Gamma = \Gamma_g \cup \Gamma_h$ in the two-dimensional space (Fig. 1) is considered. For the region, the steady incompressible Navier-Stokes equations written in terms of the stream function and vorticity, and the energy equation in a dimensionless form are

$$\vec{\nabla} \cdot (\vec{V}\omega) = \frac{1}{Re} \nabla^2 \omega \quad (1)$$

$$\nabla^2 \psi = -\omega \quad (2)$$

$$\vec{\nabla} \cdot (\vec{V}T) = \frac{1}{Pe} \nabla^2 T \quad (3)$$

where, \vec{V} is the dimensionless velocity vector with components $u = u^*/U$ and $v = v^*/U$ in the x and y directions, respectively. Also, $\omega = \omega^*L/U$ is the dimensionless vorticity, $Re = UL/\nu$ is the Reynolds number, $Pe = UL/\alpha$ is the Peclet number, $\psi = \psi^*/UL$ is the dimensionless stream function, and $T = (T^* - T_{BW})/(T_{TW} - T_{BW})$ is the dimensionless temperature.

In the meshless local Petrov-Galerkin method with unity as the test function, hereafter named the meshless control volume method (MCVM), due to its similarity with the finite volume techniques, a collection of points is selected in the domain. Subsequently, a control volume is generated around each of the points. The control volumes have simple shapes such as circle or rectangle in the two-dimensional space. The size of the control volumes and the number of points belonging to each one of them can, in general, vary. Contrary to the usual control volume techniques, in this method the control volumes can intersect each other and overlap [Versteeg and Malalasekera (1995)].

2.1 Weak formulation

To develop the vorticity, stream function, and energy weak formulations for the numerical implementation of the MCVM, Eqs. 1, 2, and 3, are multiplied by the test function w . With $w=1$ the resulting expressions are then integrated over a typical control volume Ω_i . However, in order to obtain stable solutions for convection-dominated flows, a streamline upwind scheme is required

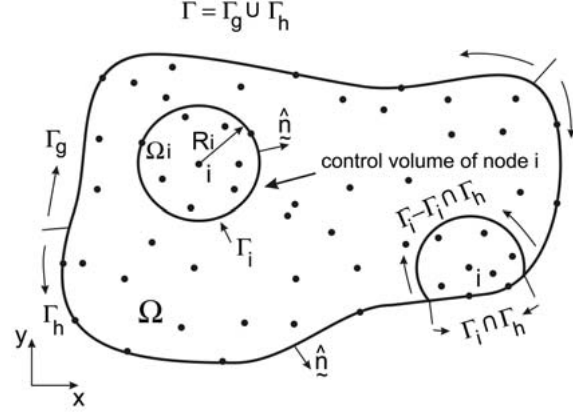


Figure 1: Domain Ω with two circular control volumes

[Brooks and Hughes (1982); Heinrich and Pepper (1999)]. Two upwinding schemes have been employed by Lin and Atluri (2000, 2001) while using the MLPG method for solving the convection-diffusion and Navier-Stokes equations. The first scheme, which is based on using different trial and test functions, is implemented through skewing the test function opposite to the streamline direction. In the second scheme, the local subdomain is moved opposite to the streamline direction when implementing the integration. The upwinding scheme employed in this study is based on adding a proper amount of artificial viscosity along the streamline direction to the governing equations. To apply the upwind technique to Eqs. 1 and 3, these equations are first transformed to the streamline coordinates, s - t , with s pointing in the streamline direction and t being perpendicular to it. The resulting equations, after adding the proper artificial viscosity $1/\overline{Re}$ and diffusivity $1/\overline{Pe}$, are

$$V \frac{\partial \omega}{\partial s} = \left(\frac{1}{Re} + \frac{1}{\overline{Re}} \right) \frac{\partial^2 \omega}{\partial s^2} + \frac{1}{Re} \frac{\partial^2 \omega}{\partial t^2} \quad (4)$$

$$V \frac{\partial T}{\partial s} = \left(\frac{1}{Pe} + \frac{1}{\overline{Pe}} \right) \frac{\partial^2 T}{\partial s^2} + \frac{1}{Pe} \frac{\partial^2 T}{\partial t^2} \quad (5)$$

where, $V = (u^2 + v^2)^{1/2}$ is the magnitude of the velocity vector. The optimal artificial viscosity and diffusivity are respectively obtained from [Arefmanesh, Najafi and Abdi (2005); Heinrich

and Pepper (1999)]

$$\frac{1}{\overline{Re}} = \frac{V\bar{h}}{2} \left[\coth\left(\frac{Re^+}{2}\right) - \frac{2}{Re^+} \right] \quad (6)$$

$$\frac{1}{\overline{Pe}} = \frac{V\bar{h}}{2} \left[\coth\left(\frac{Pe^+}{2}\right) - \frac{2}{Pe^+} \right] \quad (7)$$

where, $Re^+ = V\bar{h}/\nu$ and $Pe^+ = V\bar{h}/\alpha$ are the local Reynolds and Peclet numbers, respectively. The magnitude of \bar{h} for non-uniform point distribution cases, is $\bar{h} = (l_1|u| + l_2|v|)/V$ with l_1 and l_2 being the size of a control volume in x and y directions, respectively. Next, Eqs. 4 and 5 are transformed back to the original coordinates, x-y. The resulting equations are

$$u \frac{\partial \omega}{\partial x} + v \frac{\partial \omega}{\partial y} = \frac{1}{Re} \left(\frac{\partial^2 \omega}{\partial x^2} + \frac{\partial^2 \omega}{\partial y^2} \right) + \frac{1}{\overline{Re}V^2} \left(u^2 \frac{\partial^2 \omega}{\partial x^2} + 2uv \frac{\partial^2 \omega}{\partial x \partial y} + v^2 \frac{\partial^2 \omega}{\partial y^2} \right) \quad (8)$$

$$u \frac{\partial T}{\partial x} + v \frac{\partial T}{\partial y} = \frac{1}{Pe} \left(\frac{\partial^2 T}{\partial x^2} + \frac{\partial^2 T}{\partial y^2} \right) + \frac{1}{\overline{Pe}V^2} \left(u^2 \frac{\partial^2 T}{\partial x^2} + 2uv \frac{\partial^2 T}{\partial x \partial y} + v^2 \frac{\partial^2 T}{\partial y^2} \right). \quad (9)$$

Multiplying Eqs. 2, 8, and 9 by the test function, $w=1$, and integrating the resulting equations over Ω_i give, after integration by parts, the following weak forms of the vorticity, stream function, and energy equations for a typical control volume, respectively,

$$\int_{\Gamma_i} \vec{V} \omega \cdot \hat{n} d\Gamma = \frac{1}{Re} \int_{\Gamma_i} \frac{\partial \omega}{\partial n} d\Gamma + \frac{1}{\overline{Re}} \int_{\Gamma_i} \left(u \frac{\partial \omega}{\partial x} + v \frac{\partial \omega}{\partial y} \right) \frac{\vec{V}}{V^2} \cdot \hat{n} d\Gamma \quad (10)$$

$$\int_{\Gamma_i} \frac{\partial \psi}{\partial n} d\Gamma = - \int_{\Omega_i} \omega d\Omega \quad (11)$$

$$\int_{\Gamma_i} \vec{V} T \cdot \hat{n} d\Gamma = \frac{1}{Pe} \int_{\Gamma_i} \frac{\partial T}{\partial n} d\Gamma + \frac{1}{\overline{Pe}} \int_{\Gamma_i} \left(u \frac{\partial T}{\partial x} + v \frac{\partial T}{\partial y} \right) \frac{\vec{V}}{V^2} \cdot \hat{n} d\Gamma \quad (12)$$

where, Γ_i is the boundary of the Ω_i , and \hat{n} is the unit outward normal to the Γ_i . After solving for the stream function and the vorticity, through the following equation the appropriate pressure values can be obtained,

$$\int_{\Gamma_i} \frac{\partial P}{\partial n} d\Gamma + \int_{\Omega_i} 2 \left[\frac{\partial^2 \psi}{\partial x^2} \frac{\partial^2 \psi}{\partial y^2} - \left(\frac{\partial^2 \psi}{\partial x \partial y} \right)^2 \right] d\Omega = 0. \quad (13)$$

2.2 Fields approximations

To obtain the discretized equations for a control volume, the unknown fields have to be approximated within the control volume. A typical control volume Ω_i which contains n points is considered for this purpose. The unknown vorticity, stream function, and temperature fields are respectively approximated within Ω_i by

$$\begin{aligned} \omega(x, y) &\cong \overline{\omega}^{(i)}(x, y) \\ &= \sum_{l=1}^m P_l(x, y) \alpha_l = \mathbf{P}^T(x, y) \boldsymbol{\alpha} \end{aligned} \quad (14)$$

$$\begin{aligned} \psi(x, y) &\cong \overline{\psi}^{(i)}(x, y) \\ &= \sum_{l=1}^m P_l(x, y) \beta_l = \mathbf{P}^T(x, y) \boldsymbol{\beta} \end{aligned} \quad (15)$$

$$\begin{aligned} T(x, y) &\cong \overline{T}^{(i)}(x, y) \\ &= \sum_{l=1}^m P_l(x, y) \gamma_l = \mathbf{P}^T(x, y) \boldsymbol{\gamma} \end{aligned} \quad (16)$$

where, $\boldsymbol{\alpha} = [\alpha_1, \alpha_2, \dots, \alpha_m]^T$, $\boldsymbol{\beta} = [\beta_1, \beta_2, \dots, \beta_m]^T$, and $\boldsymbol{\gamma} = [\gamma_1, \gamma_2, \dots, \gamma_m]^T$ are vectors of unknown coefficients, and $\mathbf{P}(x, y)$ is a known vector having m elements, $p_l(x, y)$, for $l = 1(1)m$, which are, in general, monomials [Onate, Indelsohn, Zienkiewicz and Taylor (1996)]. For example, for linear approximations of the field variables, m is equal to 3 and the transpose of the vector $\mathbf{P}(x, y)$ is $\mathbf{P}^T(x, y) = [1, x, y]$.

Setting the approximations, Eqs. 13-15, equal to the values of $\omega(x, y)$, $\psi(x, y)$, and $T(x, y)$, respec-

tively, at the n points belonging to the control volume yields

$$\boldsymbol{\omega} = \begin{Bmatrix} \omega_1 \\ \vdots \\ \omega_n \end{Bmatrix} = \begin{Bmatrix} \mathbf{P}_1^T \\ \vdots \\ \mathbf{P}_n^T \end{Bmatrix} \boldsymbol{\alpha} = \mathbf{C}\boldsymbol{\alpha} \quad (17)$$

$$\boldsymbol{\psi} = \begin{Bmatrix} \psi_1 \\ \vdots \\ \psi_n \end{Bmatrix} = \begin{Bmatrix} \mathbf{P}_1^T \\ \vdots \\ \mathbf{P}_n^T \end{Bmatrix} \boldsymbol{\beta} = \mathbf{C}\boldsymbol{\beta} \quad (18)$$

$$\mathbf{T} = \begin{Bmatrix} T_1 \\ \vdots \\ T_n \end{Bmatrix} = \begin{Bmatrix} \mathbf{P}_1^T \\ \vdots \\ \mathbf{P}_n^T \end{Bmatrix} \boldsymbol{\gamma} = \mathbf{C}\boldsymbol{\gamma} \quad (19)$$

where, $\boldsymbol{\omega}$, $\boldsymbol{\psi}$ and \mathbf{T} are, respectively, the vectors of vorticity, stream function, and temperature at the n points belonging to the control volume. The elements $\omega_j = \omega(x_j, y_j)$, $\psi_j = \psi(x_j, y_j)$, and $T_j = T(x_j, y_j)$, $j = 1(1)n$, are, respectively, the magnitude of the $\boldsymbol{\omega}$, $\boldsymbol{\psi}$, and \mathbf{T} at the point (x_j, y_j) , and $\mathbf{P}_j^T = \mathbf{P}^T(x_j, y_j)$ is the transpose of vector of monomials at this point. The elements of matrix \mathbf{C} are $C_{jl} = P_l(x_j, y_j)$, $l = 1(1)m$, and $j = 1(1)n$. If the number of points belonging to the control volume, n , is equal to the number of monomials of the vector $\mathbf{P}(x, y)$, m , the performed interpolations will be exact at the points (i.e., they will be equal to the values of the unknowns functions at the points), and the vectors $\boldsymbol{\alpha}$, $\boldsymbol{\beta}$, and $\boldsymbol{\gamma}$ will be given by

$$\boldsymbol{\alpha} = \begin{Bmatrix} \mathbf{P}_1^T \\ \vdots \\ \mathbf{P}_n^T \end{Bmatrix}^{-1} \boldsymbol{\omega} = \mathbf{C}^{-1}\boldsymbol{\omega} \quad (20)$$

$$\boldsymbol{\beta} = \begin{Bmatrix} \mathbf{P}_1^T \\ \vdots \\ \mathbf{P}_n^T \end{Bmatrix}^{-1} \boldsymbol{\psi} = \mathbf{C}^{-1}\boldsymbol{\psi} \quad (21)$$

$$\boldsymbol{\gamma} = \begin{Bmatrix} \mathbf{P}_1^T \\ \vdots \\ \mathbf{P}_n^T \end{Bmatrix}^{-1} \mathbf{T} = \mathbf{C}^{-1}\mathbf{T}. \quad (22)$$

Substituting the coefficient vectors $\boldsymbol{\alpha}$, $\boldsymbol{\beta}$, and $\boldsymbol{\gamma}$ from 20-22 into the relations 14-16, respectively,

yields the following approximations for the vorticity, stream function, and temperature within the control volume Ω_i

$$\bar{\omega}^{(i)}(x, y) = \sum_{j=1}^n \phi_j^{(i)}(x, y) \omega_j \quad (23)$$

$$\bar{\psi}^{(i)}(x, y) = \sum_{j=1}^n \phi_j^{(i)}(x, y) \psi_j \quad (24)$$

$$\bar{T}^{(i)}(x, y) = \sum_{j=1}^n \phi_j^{(i)}(x, y) T_j \quad (25)$$

where, $\phi_j^{(i)}(x, y)$ with $j=1(1)n$, are the usual interpolation function for the control volume Ω_i (i.e., Lagrange polynomials) and ω_j , ψ_j , and T_j with $j=1(1)n$, are the values of the unknown functions at the points belonging to the control volume. The interpolation functions, which satisfy the standard conditions $\phi_j^{(i)}(x_l, y_l) = \delta_{jl}$ (δ_{jl} being the Kronecker delta) are given by [Heinrich and Pepper (1999); Onate, Indelsohn, Zienkiewicz and Taylor (1996)]

$$\phi_j^{(i)}(x, y) = \sum_{l=1}^m P_l(x, y) C_{lj}^{-1}, \quad j = 1(1)n \quad (26)$$

The control volumes which are employed in this study are rectangular and contain nine points each, $n=9$, such as shown in Fig. 2.

The vector $\mathbf{P}(x, y)$, which is used in this case, has nine elements, $m=9$, and its transpose is $\mathbf{P}^T(x, y) = [1, x, y, xy, x^2, y^2, x^2y, xy^2, x^2y^2]$. Substituting this vector of monomials into Eq. 26, the biquadratic interpolation functions can be readily obtained.

If the number of points belonging to the control volume is greater than the number of monomials of the vector $\mathbf{P}(x, y)$ (i.e., $n > m$), the approximations are still given by Eqs. 23-25. However, the interpolation functions are now written as follows [Onate, Indelsohn, Zienkiewicz and Taylor (1996)]:

$$\phi_j^{(i)}(x, y) = \sum_{l=1}^m P_l(x, y) D_{lj}^{-1}, \quad j = 1(1)n \quad (27)$$

where, $\mathbf{D}^{-1} = \mathbf{A}^{-1}\mathbf{B}$, $\mathbf{A} = \sum_{j=1}^m \mathbf{P}(x_j, y_j) \mathbf{P}^T(x_j, y_j)$, and $\mathbf{B} = [\mathbf{P}(x_1, y_1), \mathbf{P}(x_2, y_2), \dots, \mathbf{P}(x_n, y_n)]$.

Substituting the approximations $\bar{\omega}^{(i)}(x,y)$, $\bar{\psi}^{(i)}(x,y)$, and $\bar{T}^{(i)}(x,y)$ for the stream function, vorticity, and temperature into Eqs. 10-12, yield the discretized equations for Ω_i . Using the same procedure for every control volume gives the system of the discretized equations for all the points within the domain. Solving the system of algebraic equations yields the unknown variables at the points. The following test cases demonstrate the implementation of the method together with the obtained results.

3 Test cases and results

Equations 10, 11, and 12 are solved for different test cases. The first test case to be considered is the non-isothermal lid-driven cavity flow. The domain, the boundary conditions, the point distribution, and a typical control volume for the driven cavity flow are shown in Fig. 2. The control volume contains nine points. The shape functions are biquadratic and the interpolation is exact. For this case a 33×33 nonuniform point distribution is employed for the numerical simulations.

For the lid-driven cavity flow, the streamlines for $Re=100$ with and without upwind are shown in Figs. 3a and 3b, respectively. As the comparison of the two figures show, upwinding contributes to the accuracy of the results for the proposed method. However, based on the computations performed for moderate Reynolds numbers for fine point distributions, results without upwinding also converge, but with higher iteration compared to when upwinding is implemented. Moreover, for course point distributions cases, the results without upwinding may diverge. It should be emphasized here that the upwinding scheme in this present study is optimal, meaning that upwinding takes place only when it is needed, and it is done for the proper amount.

Figure 4 shows a comparison of the cavity horizontal centerline velocity for $Re=100$ obtained by the MCVM, with the results of the finite element method, FEM [Reddy and Gartling (2001)]. Two uniform and one nonuniform point distributions with increasing degree of refinement have been employed for the MCVM results in this figure.

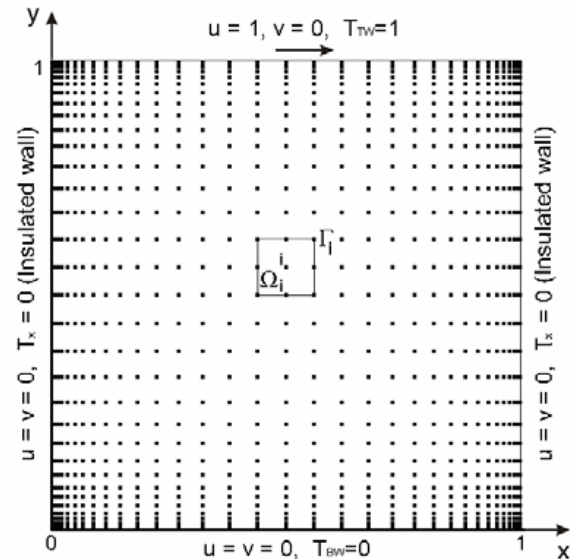


Figure 2: Domain, boundary conditions, and point distribution for non-isothermal lid-driven cavity flow

Convergence of the MCVM results to a unique velocity is also demonstrated in this figure. The converged velocity is in good agreement with the results of the finite element method. It is concluded from the results presented in this figure that a 17×17 uniform point distribution is adequate for obtaining an accurate solution in this case.

Figure 5 shows the discrete L^2 -norms of the error for the stream function and vorticity for $Re=100$ and 400. Uniform point distributions have been employed for all the results presented in this figure. The convergence of the MCVM results with decreasing the size of the control volumes is demonstrated in this figure. The rate of the convergence, as observed from the figure, is nearly quadratic. The isotherms for the driven cavity flow for the thermal boundary conditions shown in Fig. 2 for $Pe=50$ and $Re=100$, are depicted in Fig. 6.

Figures 7 and 8 show the streamlines, and the horizontal centerline velocity, respectively for the test case for $Re=400$. In Fig. 8 the horizontal centerline velocity obtained by the MCVM for different point distributions are compared with those obtained by the finite difference method

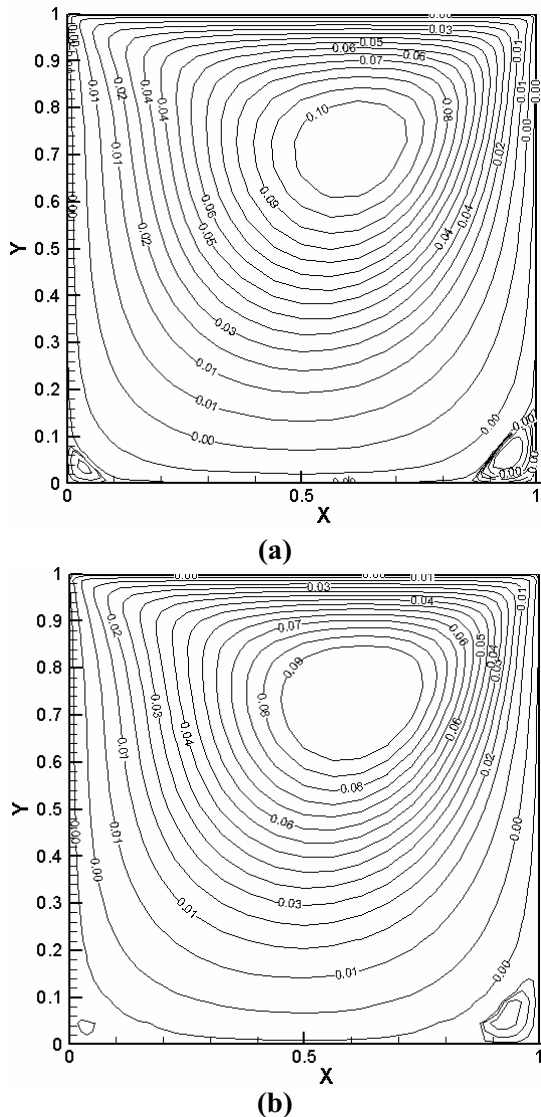


Figure 3: Streamlines for lid-driven cavity flow for $Re = 100$ a) with upwind b) without upwind

(FDM) employing a pure stream-function formulation [Kupferman (2001)]. The convergence of the MCVM results to the results of the finite difference method with decreasing the size of the control volumes is clearly observed in this figure. As both Figs. 4 and 8 (centerline velocity plots) show for Reynolds numbers 100 and 400, coarse point distributions (up to some extent), do not affect the convergence much (except for some very limited regions) compared with the existing FEM and FDM results.

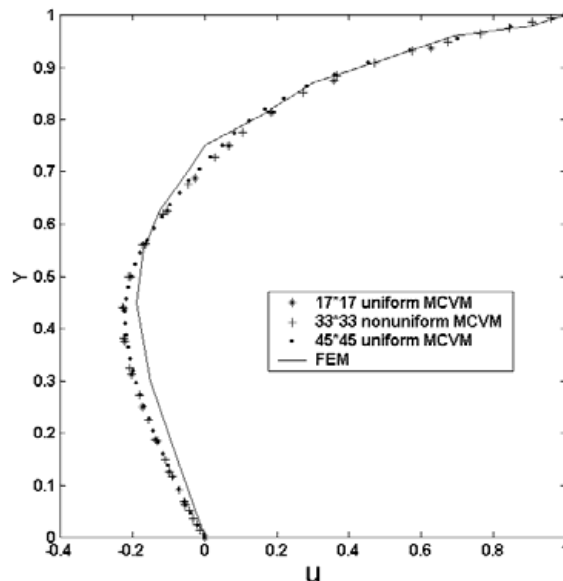


Figure 4: Cavity horizontal centerline velocities for lid-driven cavity flow for $Re = 100$, comparison of MCVM with FEM results [Reddy and Gartling (2001)]

It is emphasized here that although the proposed method is applicable for Reynolds numbers higher than 400 (of course with longer computation duration for the convergence through the iteration-scheme), Reynolds numbers 100 and 400 are utilized in this present study for comparison with the existing results by other numerical methods.

The second test case considered is the lid-driven cavity flow with an inlet and an outlet. The domain, and boundary conditions for this flow are depicted in Fig. 9. A 31×31 nonuniform point distribution is employed for the numerical simulations in this case.

The streamlines for this case for $Re=100$ is shown in Fig. 10. Figure 11 shows the discrete L^2 -norm of the error for the stream function and the vorticity. The convergence of the MCVM results with decreasing the size of the control volumes is demonstrated in this figure. Similar to the results in Fig. 5, the rate of convergence in this case is also nearly quadratic.

The non-isothermal flow over an obstacle (length

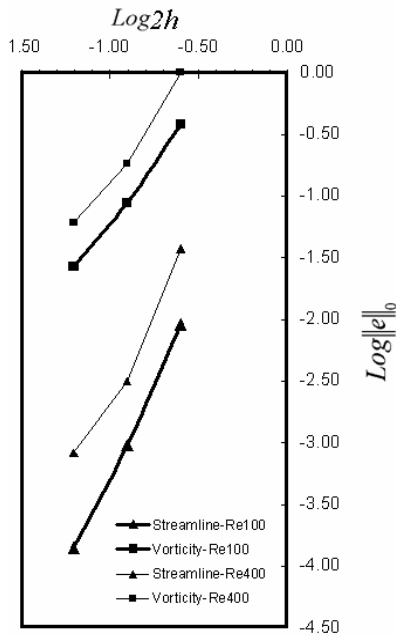


Figure 5: Discrete L^2 -norm of the error for stream function and vorticity for lid-driven cavity flow for $Re = 100$ and 400

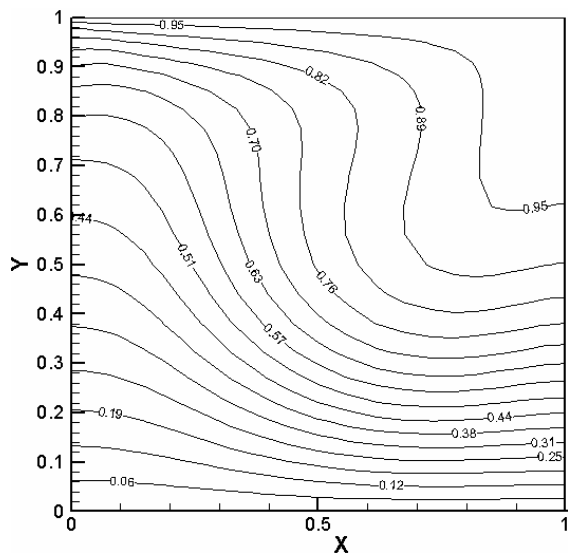


Figure 6: Isotherms for lid-driven cavity flow for $Pe = 50$ and $Re = 100$

$= 0.2$, height $= 0.3$) is considered as another test case. The domain, and the boundary conditions for this flow are shown in Fig. 12. A 107×24 nonuniform point distribution is used for the numerical simulations in this case.

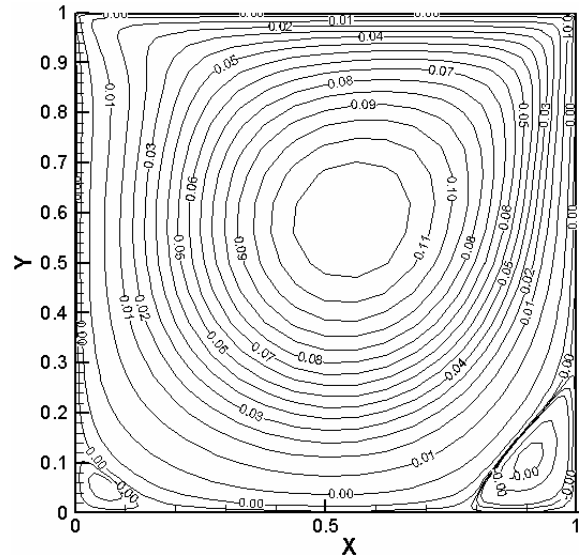


Figure 7: Streamlines for the lid-driven cavity flow for $Re = 400$

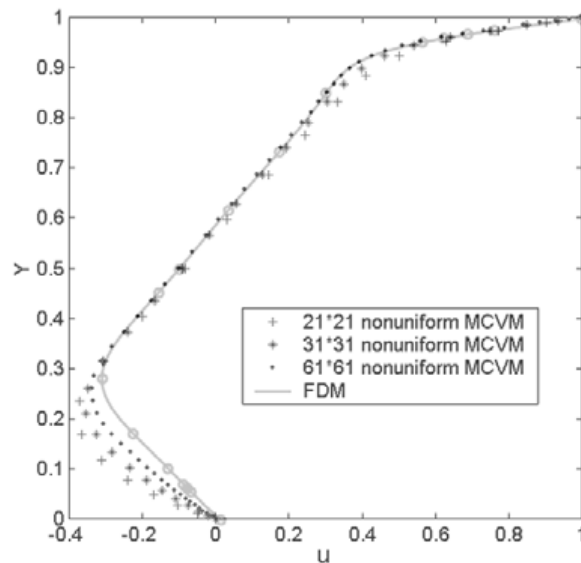


Figure 8: Cavity horizontal centerline velocity for lid-driven cavity flow for $Re = 400$, comparisons of MCVM with FDM results [Kupferman (2001)]

The streamlines and isotherms for the non-isothermal flow over an obstacle for $Pe=3$, and $Re=30$ are shown in Figs. 13 and 14, respectively. It is clear from the streamline contours that the outflow boundary condition has been properly enforced. Comparison of the MCVM results with the results obtained using a typical finite volume

the lid-driven cavity flow with one inlet and outlet. Nonuniform point distribution was utilized for all the test cases considered for the numerical simulations.

Through the method, the flow streamlines depiction was obtained for each test case. The proposed method captured the vortices distinctively for all the cases indicating the accuracy of the method.

For different Reynolds numbers, the horizontal centerline velocity for the lid-driven cavity flow was compared with the results of the other numerical techniques. The comparison show close agreements for substantial portions of the entire domains considered.

Considering both the lid-driven cavity flow and the flow over the obstacle cases, the resulting isotherms match the designated boundary conditions, showing the method accuracy.

The discrete L^2 -norms of the error for stream function and vorticity plotted for the lid-driven cavity flow with and without the inlet-outlet show nearly quadratic convergence rate.

Based on the overall results of this proposed numerical meshless method, and their comparisons with other existing numerical techniques the accuracy of the MCVM solution is established, hence the method proves to be applicable for solving non-isothermal fluid flow problems.

References

- Arefmanesh, A.; Najafi, M; Abdi, H.** (2005): A meshless local Petrov-Galerkin method for fluid dynamics and heat transfer applications, *J. of Fluids Eng.*, vol. 127, pp. 647-655.
- Atluri, S.N.** (2004): *The meshless method (MLPG) for domain and bie discretization*, Tech. Science Press, USA.
- Atluri, S. N.; Han, Z. D.; Rajendran, A. M.** (2004): A new implementation of the meshless finite volume method, through the MLPG “mixed” approach, *CMES: Computer Modeling in Engineering & Science*, vol. 6, no. 6, pp. 491-514.
- Atluri, S. N.; Liu, H. T.; Han, Z. D.** (2006): Meshless local Petrov-Galerkin (MLPG) mixed collocation method for elasticity problems, *CMES: Computer Modeling in Engineering & Science*, vol. 14, no. 3, pp. 141-152.
- Atluri, S. N.; Liu, H. T.; Han, Z. D.** (2006): Meshless local Petrov-Galerkin (MLPG) mixed finite difference method for solid mechanics, *CMES: Computer Modeling in Engineering & Science*, vol. 15, no. 1, pp. 1-16.
- Atluri, S.N.; Shen, S.** (2002): *The meshless local Petrov-Galerkin (MLPG) method*, Tech. Science Press, USA.
- Atluri, S.N.; Shen, S.** (2002): The Meshless Local Petrov-Galerkin (MLPG) Method: A Simple and Less-costly Alternative to the Finite Element and Boundary Element Methods, *CMES: Computer Modeling in Engineering & Science*, vol. 3, no. 1, pp. 11-52.
- Atluri, S.N.; Zhu, T.** (2000): The local Petrov-Galerkin (MLPG) approach for solving problems in elasto-statics, *Comput. Mech.*, vol. 25, pp. 169-179.
- Belytschko, T.; Krongauz, Y.; Organ, D.; Flemming, M.; Krysl, P.** (1996): Meshless methods: an overview and recent developments, *Comput. Methods Appl. Mech. Eng.*, vol. 139, pp. 3-47.
- Brooks, A.N.; Hughes, T.J.R.** (1982): Streamline upwind/Petrov-Galerkin formulation for convection dominated flows with particular emphasis on the incompressible Navier-Stoks equations, *Comp. Methods Appl. Mech. Eng.*, vol. 32, pp. 199-258.
- Ching, H.K.; Chen, J. K.** (2006): Thermomechanical analysis of functionally graded composites under laser heating by the MLPG method, *CMES: Computer Modeling in Engineering & Science*, vol. 13, no. 3, pp. 199-218.
- De, S.; Bathe, K.J.** (2001): The method of finite spheres with improved numerical integration, *Comput. & Truct.*, vol. 79, pp. 2183-2196.
- Gu, Y.T.; Liu, G.R.** (2001): A local point interpolation method for static and dynamic analysis of thin beams, *Comput. Methods Appl. Mech. Eng.*, vol. 190, pp. 5515-5528.
- Han, Z. D.; Atluri, S. N.** (2004): Meshless Local Petrov-Galerkin (MLPG) approaches for solving

3D Problems in elasto-statics, *CMES: Computer Modeling in Engineering & Science*, vol. 6, no. 2, pp. 169-188.

Han, Z. D.; Atluri, S. N. (2004): A meshless local Petrov-Galerkin (MLPG) approach for 3-dimensional elasto-dynamics, *CMC: Computers, Materials & Continua*, vol. 1, no. 2, pp. 129-140.

Han, Z. D.; Liu, H. T.; Rajendran, A. M.; Atluri, S. N. (2006): The applications of meshless local Petrov-Galerkin (MLPG) approaches in high-speed impact, penetration and perforation problems, *CMES: Computer Modeling in Engineering & Science*, vol. 14, no. 2, pp. 119-128.

Han, Z. D.; Rajendran, A. M.; Atluri, S.N. (2005): Meshless local Petrov-Galerkin (MLPG) approaches for solving nonlinear problems with large deformations and rotations, *CMES: Computer Modeling in Engineering & Science*, vol. 10, no. 1, pp. 1-12.

Heinrich, J.C.; Pepper, D.W. (1999): *Intermediate finite element method*, Taylor and Francis, USA.

Hu, D.A.; Long, S.Y.; Liu, K.Y.; Li, G.Y. (2006): A modified meshless local Petrov-Galerkin method to elasticity problems in computer modeling and simulation, *Eng. Analysis Boundary Elem.*, vol. 30, no. 5, pp. 399-404.

Jarak, T.; Sorić, J.; Hoster, J. (2007): Analysis of shell deformation responses by the meshless local Petrov-Galerkin (MLPG) approach, *CMES: Computer Modeling in Engineering & Science*, vol. 18, no. 3, pp. 235-246.

Johnson, J.N.; Owen, J.M. (2007): A Meshless Local Petrov-Galerkin Method for Magnetic Diffusion in Non-magnetic Conductors, *CMES: Computer Modeling in Engineering & Science*, vol. 22, no. 3, pp. 165-188.

Kupferman, R. (2001): A central-difference scheme for a pure stream function formulation of incompressible viscous flow, *SIAM J. Sci. Comput.*, vol. 23, No. 1, pp 1-18.

Liu, L.H. (2006): Meshless method for radiation heat transfer in graded index medium, *Int. J. Heat Mass Transfer*, vol. 49, pp. 219-229.

Lin, H.; Atluri, S.N. (2001): The meshless lo-

cal Petrov-Galerkin (MLPG) method for solving incompressible Navier-Stokes equations, *CMES: Computer Modeling in Engineering & Science*, vol. 2, no. 2, pp. 117-142.

Lin, H.; Atluri, S.N. (2000): Meshless local Petrov-Galerkin (MLPG) method for convection-diffusion problems, *CMES: Computer Modeling in Engineering & Science*, vol. 1, no. 2, pp. 45-60.

Lu, Y.Y.; Belytschko, T.; and Gu, L. (1994): A new implementation of the element-free Galerkin method, *Comput. Methods Appl. Mech. Eng.*, vol. 113, pp. 397-414.

Ma, Q.W. (2005): MLPG method based on Rankine source solution for simulating nonlinear water waves, *CMES: Computer Modeling in Engineering & Science*, vol. 9, no.2, pp. 193-210.

Nayrols, B.; Touzot, G.; Villon, P. (1992): Generalizing the FEM: Diffuse Approximation and Diffuse Elements, *Comput. Mech.*, vol. 10, pp. 307-318.

Onate, E.; Indelsohn, S.; Zienkiewicz, O.C., and Taylor, R. (1996): A finite point method in computational mechanics: applications to convective transport and fluid flow, *Int. J. Numer. Methods Eng.*, vol. 39, pp. 3839-3866.

Patankar, S.V. (1980): *Numerical heat transfer and fluid flow*, Hemisphere Publishing Corp., USA.

Reddy, J.N.; Gartling, D.K. (2001): *The finite element method in heat transfer and fluid dynamics*, CRC Press.

Sellountos, E. J.; Vavourakis, V.; Polyzos, D. (2005): A new singular/hypersingular MLPG (LBIE) method for 2D elastostatics, *CMES: Computer Modeling in Engineering & Science*, vol. 7, no. 1, pp. 35-48.

Sladek, J.; Sladek, V.; Atluri, S.N. (2004): Meshless local Petrov-Galerkin method in anisotropic elasticity, *CMES: Computer Modeling in Engineering & Science*, vol. 6, no. 5, pp. 477-490.

Sladek, J.; Sladek, V.; Atluri S.N. (2004): Meshless local Petrov-Galerkin method for heat conduction problem in an anisotropic medium,

CMES: Computer Modeling in Engineering & Science, vol. 6, no. 3, pp. 309-318.

Sladek, J.; Sladek, V.; Wen, P. H.; Aliabadi, M.H. (2006): Meshless local Petrov-Galerkin (MLPG) method for shear deformable shells analysis, *CMES: Computer Modeling in Engineering & Science*, vol. 13, no. 2, pp. 103-118.

Sladek, J.; Sladek, V.; Zhang, Ch.; Solek, P. (2007): Application of the MLPG to Thermo-Piezoelectricity, *CMES: Computer Modeling in Engineering & Science*, vol. 22, no. 3, pp. 217-234.

Sladek, J.; Sladek, V.; Zhang, Ch.; Solek, P.; Starek, L. (2007): Fracture analyses in continuously nonhomogeneous piezoelectric solids by the MLPG, *CMES: Computer Modeling in Engineering & Science*, vol. 19, no. 3, pp. 247-262.

Sorić, J.; Li, Q.; Jarak, T.; Atluri, S.N. (2004): Meshless Local Petrov-Galerkin (MLPG) Formulation for Analysis of Thick Plates, *CMES: Computer Modeling in Engineering & Science*, vol. 6, no. 4, pp. 349-358.

Vavourakis, V.; Polyzos, D. (2007): A MLPG4 (LBIE) formulation in elastostatics, *CMC: Computers, Materials & Continua*, vol. 5, no. 3, pp. 185-196.

Vavourakis, V.; Sellountos, E. J.; Polyzos, D. (2006): A comparison study on different MLPG(LBIE) formulations, *CMES: Computer Modeling in Engineering & Science*, vol. 13, no. 3, pp. 171-184.

Versteeg, H.K.; Malalasekera, W. (1995): *An introduction to computational fluid dynamics, the finite volume method*, Longman, Loughborough, England.

Wu, X.; Shen, S.; Tao W. (2007): Meshless Local Petrov-Galerkin Collocation Method for Two-dimensional Heat Conduction Problems, *CMES: Computer Modeling in Engineering & Science*, vol. 22, no. 1, pp. 65-76.

Zhang, J.; Yao, Z. (2004): The regular hybrid boundary node method for three-dimensional linear elasticity, *Eng. Analysis Boundary Elem.*, vol. 28, pp. 525-534.

Zhu, T.; Zhang, T. D.; Atluri, S. N. (1998): A

meshless local boundary integral equation (LBIE) method for solving nonlinear problems, *Comput. Mech.*, vol. 22, pp. 174-186.